

Synthesis and Characterization of Ferromagnetic Polyaniline with Conductivity in an Applied Magnetic Field

Ya Zhang, Chunxia Zhu, Jinqing Kan

School of Chemistry and Chemical Engineering, Yangzhou University, Yangzhou 225002, People's Republic of China

Received 31 July 2007; accepted 18 March 2008

DOI 10.1002/app.28414

Published online 20 May 2008 in Wiley InterScience (www.interscience.wiley.com).

ABSTRACT: Ferromagnetic polyaniline (PANI) with conductivity was synthesized with peroxydisulfate as an oxidant and horseradish peroxidase as a catalyst in an *N'*-*a*-hydroxythylpiperazine-*N'*-ethanesulfonic acid buffer solution containing aniline, HCl, and NiCl₂·6H₂O in an applied magnetic field. The result of an electron paramagnetic resonance spectrum indicated that there were unpaired electrons in the resulting product, the spin density of which was 7.60×10^{19} spins/g. The curve of the magnetization versus the magnetic field showed that PANI had soft ferromagnetic behavior at about 300 K. The saturation mag-

netization and coercive force of PANI were 0.033 emu/g and 5 Oe, respectively. Ultraviolet–visible and Fourier transform infrared spectra indicated that there was interaction between Ni²⁺ and PANI chains but the structure of the backbone chains of PANI synthesized in the presence of a magnetic field hardly changed compared with that of PANI synthesized without NiCl₂·6H₂O. © 2008 Wiley Periodicals, Inc. *J Appl Polym Sci* 109: 3024–3029, 2008

Key words: conjugated polymers; ESR/EPR; ferroelectricity; FT-IR; magnetic polymers

INTRODUCTION

Magnetic materials have been widely used and play an important role in many areas, such as magnetic drug targeting, spacecraft, precision instruments, optical communications, sensors, and electronic devices.^{1–6} Organic ferromagnetism has received a great deal of interest because of its structural diversification, low density, and easy processing.^{7,8} The pure organic ferromagnet is still a challenge because its Curie temperature is too low for practical use.⁹

From a practical point of view, researchers have proposed a strategy including composites containing a polymer matrix and ferromagnetic inorganic particles.^{10–14} However, phase separation is a common phenomenon in composites that are generally a multiphase system.^{15,16} Conducting polymers have recently emerged as materials of great potential because of their rare combination of useful properties, such as interesting optical behavior, mechanical properties, and metallic or semiconducting properties.

To overcome the drawbacks of both pure organic ferromagnetism and composite ferromagnets with

conductivity, we suggest a novel and easy strategy of synthesizing a complex polymer with both conductive and ferromagnetic magnets in the presence of metal ions. There are unpaired electrons and vacant orbits in some metal ions,¹⁷ and there are donating abilities of the lone pair of electrons on the nitrogen or sulfur atoms in conducting polymer chains.¹⁸ When metal ions are added to the synthesized system of a conducting polymer, the metal ions can complex with the nitrogen atoms or sulfur in conducting polymer chains. This idea has been partially confirmed by both the experimental results of a polyaniline (PANI) base doped with high-spin Fe³⁺¹⁹ and the influence of an applied magnetic field on a chemical reaction containing molecules of unpaired electrons.²⁰ The existence of paramagnetic ions (e.g., rare-earth ions³⁺) in solutions can greatly increase the effects of magnetic alignment.²¹ The dynamics of domain walls under the action of an applied magnetic field are responsible for most magnetic properties, such as hysteresis loops, coercivity, and magnetization noise.²²

In this article, we report a simple method for the chemical synthesis of ferromagnetic PANI with conductivity in the presence of both NiCl₂·6H₂O and an applied magnetic field. The interaction between Ni²⁺ and the nitrogen atoms in the PANI chains was confirmed by IR and ultraviolet–visible (UV–vis) spectra. The PANI had a high conductivity and ferromagnetic behavior at ambient temperature.

Correspondence to: J. Kan (jqkan@yzu.edu.cn).

Contract grant sponsor: National Science Foundation of China; contract grant number: 20673095.

EXPERIMENTAL

Chemicals

The aniline monomer (reagent-grade) was purified into colorlessness by reduced-pressure distillation and stored in a refrigerator. Ammonium peroxydisulfate, *N,N*-dimethylformamide (DMF), *N'*-*a*-hydroxythylpiperazine-*N'*-ethanesulfonic acid, $\text{NiCl}_2 \cdot 6\text{H}_2\text{O}$, and other chemicals were reagent grade and were used as received without further treatment. All of the aqueous solutions were prepared with doubly distilled water.

Synthesis

PANI was synthesized in 100 cm^{-3} of a solution containing 0.5 mol/dm^3 HCl, 0.1 mol/dm^3 aniline, 4 mg of horseradish peroxidase, and 2.4036 g of *N'*-*a*-hydroxythylpiperazine-*N'*-ethanesulfonic acid with $\text{NiCl}_2 \cdot 6\text{H}_2\text{O}$ in the presence of a magnetic field (500 mT). The magnetic field was applied by a home-made permanent magnet. Ammonium peroxydisulfate with the same molar ratio as aniline was added to the solution at about 0.15 g/min while the solution was stirred in ultrasonicator. The chemical polymerization of aniline was carried out at 30°C , and the reactive time was 24 h. After the reaction, the products were separated by filtration, washed with doubly distilled water and ethanol, and then dried at 65°C for 24 h.

Apparatus

The UV-vis spectra of all samples were obtained with a UV-2550 spectrometer (Shimadzu, Japan) in the range 250–900 nm. DMF was used as the solvent. Fourier transform infrared (FTIR) spectra of those samples were obtained with a Tensor 27 FTIR spectrometer (Bruker, Germany) in KBr pellets. The morphology of PANI was observed with a Tecnai-12 transmission electron microscope (Philips, Holland). The PANI films were formed as follows: first, the powder of PANI was dispersed in ethanol in ultrasonicator; then, the solution was spread on a copper net. The conductivity of the resulting products was measured with a standard four-probe method. The standard deviation was less than 2.0% in our experiments with an YJ8312 model current source (Shanghai Huguang Instrument Works, China) and M92A digital multimeter (Mastech, China). Wide-angle X-ray diffraction patterns for the powder samples were taken on a M03XHF²² diffractometer (Mac Science, Japan) with Cu $K\alpha$ radiation ($\lambda = 1.541 \text{ \AA}$). The hysteresis loops were obtained on a vibrating sample magnetometer (EV7, ADE, USA). The electron paramagnetic resonance (EPR) measurements were carried out with an A300-10/12 spectrometer (Bruker) operating in the X band (9.856 GHz). The microwave power for the

measures was 0.2 mW, and the modulation amplitude was set at 2.00G.

RESULTS AND DISCUSSION

EPR spectra

Figure 1 shows the EPR spectrum of PANI synthesized with $\text{NiCl}_2 \cdot 6\text{H}_2\text{O}$ in the presence of an applied magnetic field. The EPR spectra of PANI synthesized with $\text{NiCl}_2 \cdot 6\text{H}_2\text{O}$ in the absence of an applied magnetic field (sample B) and without $\text{NiCl}_2 \cdot 6\text{H}_2\text{O}$ (sample C) were very similar to that of Figure 1 (here omitted). The g values of samples A and B were both 2.0034, which were close to the value of the free electron (2.0023). This indicated that there were unpaired electrons in the PANI, which is one of the forming conditions of ferromagnetism. The spin densities of the samples were calculated on the basis of 1.53×10^{21} spins/g of diphenyl picryl hydrazil and their peak areas of the EPR spectra. The spin densities of samples A and B were 7.60×10^{19} and 1.09×10^{19} spins/g, respectively. As a comparison, the spin density of sample C was on the magnitude of 10^{18} spins/g, which was in agreement with the literature.²³ The spin density of samples A and B were more than that of sample C; the appropriate explanations are as follows: (1) the spins for both samples A and B may have partially come from the unpaired electrons in Ni^{2+} , and (2) interaction between Ni^{2+} and the PANI chain made the PANI chains aggregate more closely together. The spin density of sample A was more than that of sample B, which indicated that the applied magnetic field decreased the charge delocalization in PANI by making the PANI chains twist.

Magnetic properties and conductivity

The magnetic properties of the PANI samples synthesized with $\text{NiCl}_2 \cdot 6\text{H}_2\text{O}$ were investigated at room

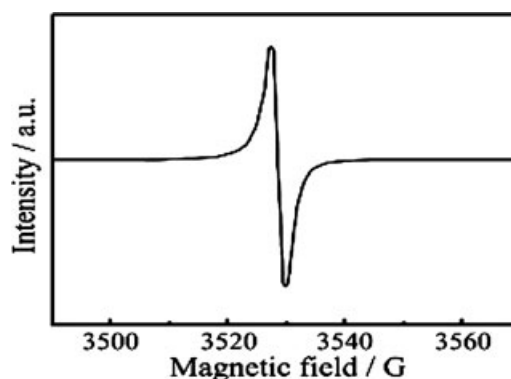


Figure 1 EPR spectra of PANI synthesized with $\text{NiCl}_2 \cdot 6\text{H}_2\text{O}$ at 500 mT.

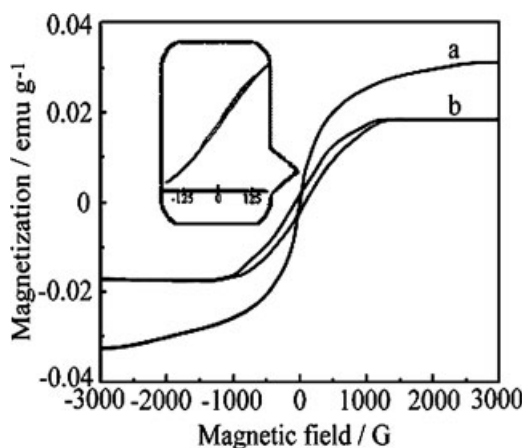


Figure 2 Magnetization/applied magnetic field plot of PANI synthesized in the (a) presence and (b) absence of a magnetic field.

temperature with a vibrating sample magnetometer. Figure 2(a,b) shows the plots of magnetization against an applied magnetic field for samples A and B, respectively. The inset in Figure 2 is the magnification of the middle part of the magnetization/applied magnetic field plot of sample A. Both samples A and B clearly exhibited hysteresis loops at about 300 K. According to the result of XPS, there was only a trace amount of nickel in the PANI, so the nickel ions could not contribute to the ferromagnetic properties of the PANI by calculation. The ferromagnetic properties must not also come from $\text{NiCl}_2 \cdot 6\text{H}_2\text{O}$ because $\text{NiCl}_2 \cdot 6\text{H}_2\text{O}$ was only paramagnetic at room temperature. It is well known that two conditions have to be satisfied for ferromagnetism: an unpaired electron must be contained, and the orientation between unpaired electrons must be parallel to aggregate into magnetic domains.²⁴ Bi et al.²⁵ reported that Co^{2+} ions may bind to more than one nitrogen site in a PANI chain or form interchain linkages among several adjacent PANI chains by coordination; both intrachain and interchain connections may lead to a more coil-like conformational change or a more twisted aggregation of PANI chains. The electron configuration of Ni^{2+} was similar to that of Co^{2+} . It was deduced that the interaction between Ni^{2+} and the PANI chains might have been favorable to the formation of a ferromagnetic domain. To further understand the forming mechanism of ferromagnetic PANI with conductivity, we suggest a forming process of ferromagnetic PANI (Fig. 3).

According to Figure 2, the saturation magnetization of samples A and B were 0.033 and 0.018 emu/g, respectively; their coercive forces were about 5 and 55 Oe, respectively. Unfortunately, the image resolution of sample A was too low to be visible in Figure 2. The low values of the coercive force indi-

cated that the ferromagnetic PANI was a soft ferromagnetic material.²⁶ Compared with sample B, sample A had a higher saturation magnetization. Li et al.²⁷ reported that the saturation magnetization depended on the weight fraction of the magnetic compound. This indicated that the applied magnetic field could have made the weight fraction of the ferromagnetic in PANI rise. At the same time, the smaller coercive force of sample A may have been due to the twist of the PANI chains in the applied magnetic field. However, the detailed mechanism of the coercive force decrease of PANI synthesized in the applied magnetic field was left unclarified.

The conductivities of samples A and B were 0.066 and 0.22 S cm^{-1} , respectively. That is, the applied magnetic field was unfavorable for the improvement of the conductivity of the PANI. The reason may have been that the applied magnetic field made the conformation of PANI chains deform, so the decrease of charge delocalization in PANI resulted in a decrease in the conductivity; this result was in agreement with the literature.²⁵

UV-vis spectra and FTIR spectra

Figure 4 shows the UV-vis absorption spectra of PANI dissolved in DMF. PANI was synthesized without $\text{NiCl}_2 \cdot 6\text{H}_2\text{O}$ [Fig. 4(a)] and with $\text{NiCl}_2 \cdot 6\text{H}_2\text{O}$ in the absence [Fig. 4(b)] and presence [Fig. 4(c)] of an applied magnetic field. As shown in Figure 4, in all samples, there existed two absorption bands, one

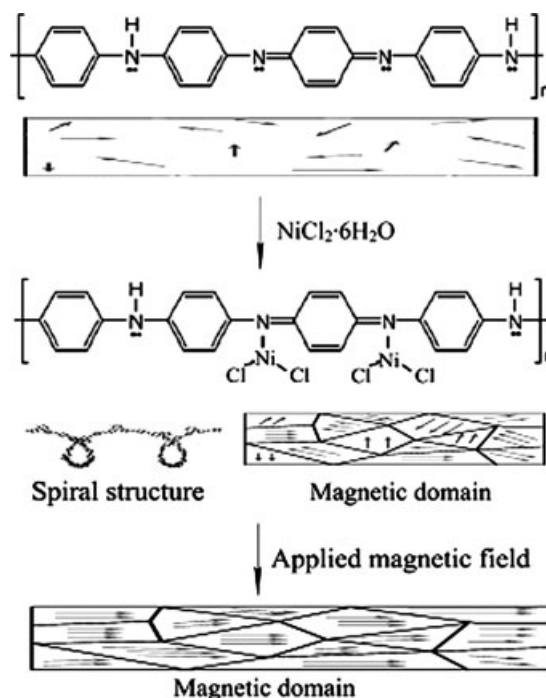


Figure 3 Possible forming mechanism of ferromagnetic PANI.

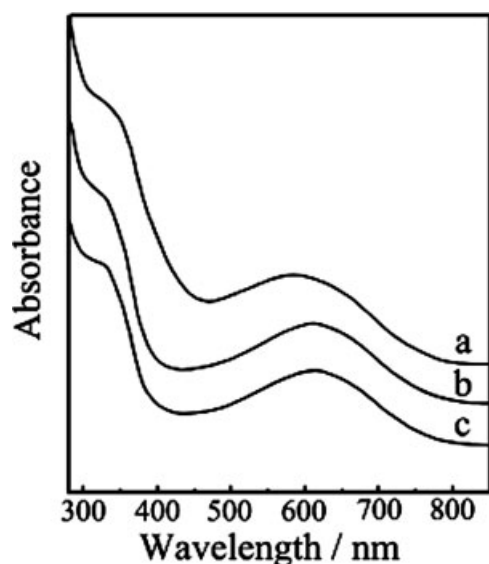


Figure 4 UV-vis spectra of the products: (a) PANI synthesized without $\text{NiCl}_2 \cdot 6\text{H}_2\text{O}$, (b) PANI synthesized with $\text{NiCl}_2 \cdot 6\text{H}_2\text{O}$, and (c) PANI synthesized with $\text{NiCl}_2 \cdot 6\text{H}_2\text{O}$ at 500 mT.

at about 350 nm and the other at about 600 nm. The 350-nm absorption band was assigned to the $\pi\text{-}\pi^*$ transition,^{28–31} and the 600-nm absorption band was assigned to the quinoid ring transition in the chain of PANI.^{31,32}

By comparison with that of PANI synthesized without $\text{NiCl}_2 \cdot 6\text{H}_2\text{O}$ [Fig. 4(a)], we found that the absorption peak due to the quinoid ring transition in Figure 4(b,c) shifted to longer wavelengths, which were at 621 and 609 nm. These results indicated that (1) there was strong interaction between Ni^{2+} and the PANI chain,³³ and this interaction made the energy for the quinoid ring transition weaker [Fig. 4(b)] and (2) when compared with that of PANI synthesized with $\text{NiCl}_2 \cdot 6\text{H}_2\text{O}$ in the absence of an applied magnetic field [Fig. 4(b)], the peak in Figure 4(c) due to the quinoid ring transition shifted to a shorter wavelength; that is to say, the applied magnetic field made the PANI molecules distort and the charge delocalization decrease. This result was in agreement with the result of conductivity. In addition, the peaks due to the $\pi\text{-}\pi^*$ transition of all of the samples showed little shift. We inferred from the results of the UV-vis spectra that the Ni^{2+} interacted with the nitrogen atoms on the quinone ring.

Figure 5(a–c) shows the FTIR spectra of samples C, B, and A, respectively. The peaks at about 1570 and 1490 cm^{-1} were attributed to the stretching vibrations of the $\text{N}=\text{Q}=\text{N}$ ring and $\text{N}-\text{B}-\text{N}$ ring, respectively (where B refers to benzenic-type rings and Q refers to quinonic-type rings). The peak at 1350 cm^{-1} corresponded to $\text{C}-\text{N}$ stretching vibrations. The peaks at 1109 and 800 cm^{-1} were attributed to the characteristic $\text{B}-\text{NH}-\text{Q}$ or $\text{B}-\text{NH}-\text{B}$

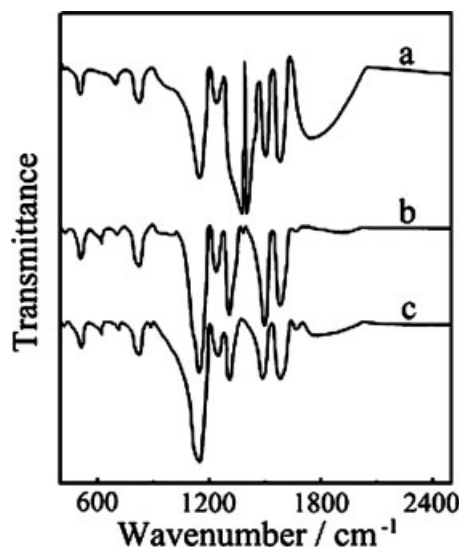


Figure 5 FTIR spectra of the products: (a) PANI synthesized without $\text{NiCl}_2 \cdot 6\text{H}_2\text{O}$, (b) PANI synthesized with $\text{NiCl}_2 \cdot 6\text{H}_2\text{O}$, and (c) PANI synthesized with $\text{NiCl}_2 \cdot 6\text{H}_2\text{O}$ at 500 mT.

bonds and out-of-plane bending vibrations of $\text{C}-\text{H}$ of benzene rings.^{34–37} The absorption band at about 1400 cm^{-1} was attributed to the sulfate anion coming from the reaction products between aniline and $\text{S}_2\text{O}_8^{2-}$.³⁸ A comparison of Figure 5(c) with Figure 5(b) showed that the peaks of the quinoid units shifted from 1578 and 1155 to 1562 and 1149 cm^{-1} , respectively. This indicated that the applied magnetic field made the peaks of the FTIR spectra appear at higher wave numbers.

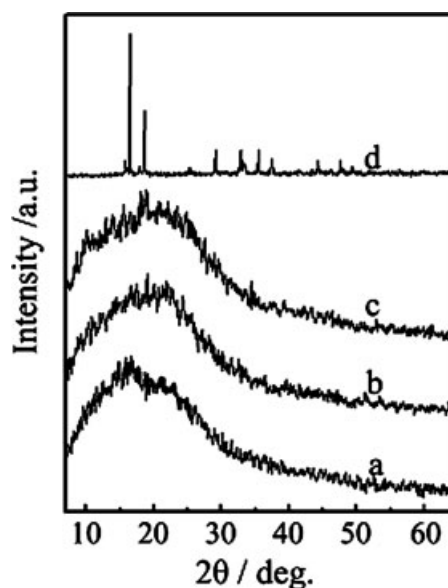


Figure 6 XRD patterns of the products: (a) PANI synthesized with $\text{NiCl}_2 \cdot 6\text{H}_2\text{O}$, (b) PANI synthesized with $\text{NiCl}_2 \cdot 6\text{H}_2\text{O}$ at 500 mT, (c) PANI synthesized without $\text{NiCl}_2 \cdot 6\text{H}_2\text{O}$, and (d) NiCl_2 .

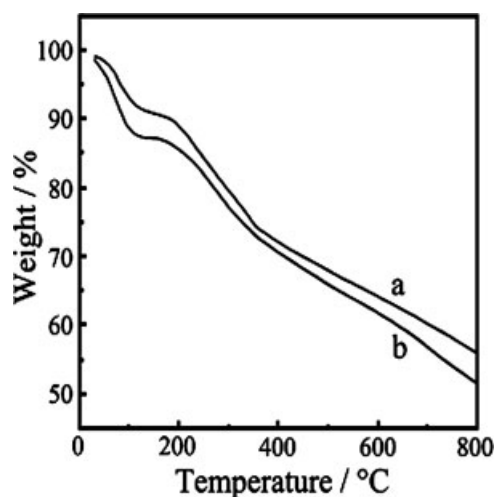


Figure 7 Thermogravimetric analysis curves of the products: (a) PANI synthesized with $\text{NiCl}_2 \cdot 6\text{H}_2\text{O}$ and (b) PANI synthesized with $\text{NiCl}_2 \cdot 6\text{H}_2\text{O}$ at 500 mT.

We inferred from the results of the UV-vis and FTIR spectra that the structures of the backbone chains of samples A and B hardly changed compared with that of sample C. So the PANIs synthesized with $\text{NiCl}_2 \cdot 6\text{H}_2\text{O}$ in the presence and absence of a magnetic field were complex polymers.

X-ray diffraction spectra

Figure 6(a–d) shows the X-ray diffractograms of samples A, B, and C and $\text{NiCl}_2 \cdot 6\text{H}_2\text{O}$, respectively. The X-ray diffractogram in Figure 6(d) shows the characteristic diffraction peaks of NiCl_2 at $2\theta = 16.5, 18.6, 29.2, 32.8, 35.5,$ and 37.5° , whereas samples A, B, and C revealed broad peaks at $2\theta = 20^\circ$. The broad structure was characteristic of diffraction by an amorphous PANI. This result was in good agreement with reported results.³⁹ Figure 6(a–c) shows

the same pattern, which indicates that the Ni^{2+} ions and applied magnetic field hardly influenced the crystallinity of the PANI.

Thermogravimetric analysis

Figure 7(a,b) shows thermogravimetric curves of samples B and A, respectively. In general, the thermal behavior of the PANI/HCl showed a three-step weight loss process; the first weight loss, from 50 to 100°C, was attributed to the loss of water and low-molecular-weight oligomers.⁴⁰ The second weight loss, ranging from 150 to 300°C, was believed to be due to the elimination of acid dopant (HCl),^{41–43} and the third weight loss, starting at about 400°C, corresponded to the thermal decomposition of PANI backbone chains.^{44,45} A comparison of Figure 7(b) with Figure 7(a) shows that the three-step weight losses exhibited similar thermal behavior in samples A and B. This indicated that the magnetic field had no remarkable effect on the thermal behavior of the PANI.

Transmission electron microscopy (TEM) morphology

Figure 8(a,b) shows the TEM morphology of PANI synthesized with $\text{NiCl}_2 \cdot 6\text{H}_2\text{O}$ in the absence and presence of an applied magnetic field, respectively. As shown in Figure 8(a), the PANI particles displayed morphologies of linked spherical particles with average size of 30–60 nm rather than the typical core-shell structure of polymer composites. Compared with that of PANI synthesized without $\text{NiCl}_2 \cdot 6\text{H}_2\text{O}$ in the absence of an applied magnetic field, the diameters of PANI particles synthesized in the presence of an applied magnetic field were larger. This might have been because the cooperative

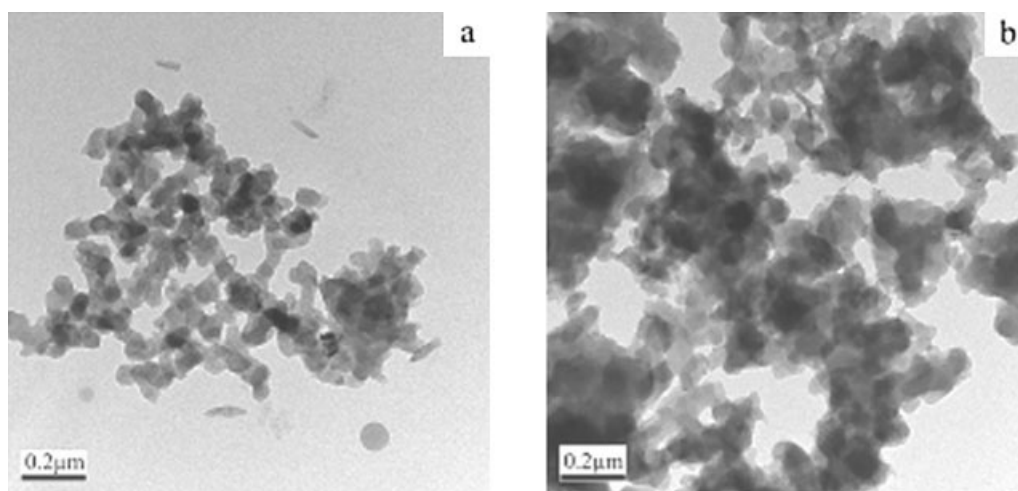


Figure 8 TEM morphology of PANI synthesized with $\text{NiCl}_2 \cdot 6\text{H}_2\text{O}$ at (a) 0 and (b) 500 mT.

effect between Ni^{2+} and the applied magnetic field favored the formation in the PANI chains of a more coil-like conformational change or a more twisted aggregation of PANI chains. However, further studies are needed on the appearance.

CONCLUSIONS

Ferromagnetic PANI with conductivity was obtained in the presence of a magnetic field and $\text{NiCl}_2 \cdot 6\text{H}_2\text{O}$. UV-vis and FTIR spectra indicated that there was interaction between Ni^{2+} and the PANI chains, but the structure of the backbone chains of PANI synthesized in the presence of the magnetic field hardly changed compared with those of PANI synthesized without $\text{NiCl}_2 \cdot 6\text{H}_2\text{O}$. The EPR spectra result indicates that there were unpaired electrons in the PANI; the spin density of the PANI was 7.60×10^{19} spins/g. The magnetization/applied magnetic field curve showed that the PANI synthesized in the presence of the magnetic field was of soft ferromagnetic behavior at about 300 K. The saturation magnetization and coercive force of the PANI synthesized in the same conditions were 0.033 emu/g and 5 Oe, respectively.

References

- Salafsky, J. S. *Phys Rev B* 1999, 59, 10885.
- Su, S. J.; Kuramoto, N. *Synth Met* 2000, 114, 147.
- Haihua, L.; Zekun, F. *J Magn Magn Mater* 2001, 237, 153.
- Zhang, L. J.; Wan, M. X. *J Phys Chem B* 2003, 107, 6748.
- Dey, A.; De, S.; De, A.; De, S. K. *Nanotechnology* 2004, 15, 1277.
- Shokrollahi, H.; Janghorban, K. *J Magn Magn Mater* 2007, 308, 238.
- Zheng, S.; Lan, J.; Khan, S. I.; Rubin, Y. *J Am Chem Soc* 2003, 125, 5786.
- Shimono, S.; Tamura, R.; Ikuma, N.; Takimoto, T.; Kawame, N.; Tamada, O.; Sakai, N.; Matsuura, H.; Yamauchi, J. *J Org Chem* 2004, 69, 475.
- Sun, X.; Xu, X. H.; Hu, K.; Yonemitsu, K. *Phys Lett A* 1998, 239, 191.
- Asefa, T.; Yoshina-Ishii, C.; MacLachlan, M. J.; Ozin, G. A. *J Mater Chem* 2000, 10, 1751.
- Boury, B.; Corriu, R. J. P. *Adv Mater* 2000, 12, 989.
- Kryszewski, M. *Synth Met* 2000, 109, 47.
- Choudhury, K. R.; Winiarz, J. G.; Samoc, M.; Prasad, P. N. *Appl Phys Lett* 2003, 82, 406.
- Schnitzler, D. C.; Meruvia, M. S.; Hummelgen, I. A.; Zarbin, A. J. G. *Chem Mater* 2003, 15, 4658.
- Manson, J. A.; Sperling, L. H. *Polymer Blends and Composites*; Plenum Press: New York, 1976.
- Wang, H. T.; Xu, P.; Meng, S.; Zhong, W.; Du, W. C.; Du, Q. G. *Polym Degrad Stab* 2006, 91, 1455.
- Xiao, H.; Morsali, A. *Solid State Sci* 2007, 9, 155.
- Trivedi, D. C. *Synth Met* 2001, 121, 1780.
- Gosk, J. B.; Kulszewicz-Bajer, I.; Twardowski, A. *Synth Met* 2006, 156, 773.
- Turro, N. J.; Chow, M. F.; Chung, C. J.; Weed, G. C.; Kraeutler, B. *J Am Chem Soc* 1980, 102, 4843.
- Stupp, I. *Sci News* 1986, 129, 297.
- Durin, G.; Colaiori, F.; Castellano, C.; Zapperi, S. *J Magn Magn Mater* 2007, 316, 436.
- Anand, J.; Palaniappan, S.; Sathyanarayana, D. N. *J Phys Chem* 1995, 99, 10324.
- Chikazumi, S.; Graham, C. D. *Physics of Ferromagnetism* (2nd ed); Oxford University Press: New York, 1997.
- Sun, T.; Bi, H.; Zhu, K. R. *Spectrochim Acta Part A* 2007, 66, 1364.
- Daigo, I.; Toshitaka, M.; Hideo, K. *J Appl Polym Sci* 1998, 70, 717.
- Li, G. J.; Yan, S. F.; Zhou, E. L.; Chen, Y. M. *Colloids Surf A* 2006, 276, 40.
- Epstein, A. J.; Ginder, J. M.; Zuo, F.; Bigelow, R. W.; Woo, H. S.; Tanner, D. B.; Richter, A. F.; Huang, W. S.; MacDiarmid, A. G. *Synth Met* 1987, 18, 303.
- Wan, M. X. *Synth Met* 1989, 31, 51.
- McManus, P. M.; Yang, S. C.; Cushman, R. J. *J Chem Soc Chem Commun* 1985, 1556.
- Li, D.; Jiang, Y. D.; Wu, Z. M.; Chen, X. D.; Li, R. *Thin Solid Films* 2000, 360, 24.
- Stafström, S.; Brédas, J. L.; Epstein, A. J.; Woo, H. S.; Tanner, D. B.; Huang, W. S.; MacDiarmid, A. G. *Phys Rev Lett* 1987, 59, 1464.
- Forsberg, J. H. *Coord Chem Rev* 1973, 10, 195.
- Stilwell, D. E.; Park, S. M. *J Electrochem Soc* 1988, 135, 2254.
- Yan, B.; Yang, J.; Li, Y.; Car, Y. *Synth Met* 1991, 44, 189.
- Hand, R. L.; Nelson, R. F. *J Am Chem Soc* 1974, 96, 850.
- Yang, C. M.; Chen, C. Y.; Zeng, Y. *Spectrochim Acta Part A* 2007, 66, 37.
- Stejskal, J.; Sapurina, I.; Trchova, M.; Prokes, J.; Krivka, I.; Tobolkova, E. *Macromolecules* 1998, 31, 2218.
- Pouget, J. P.; Jozefowicz, M. E.; Epstein, A. J.; Tang, X.; MacDiarmid, A. G. *Macromolecules* 1991, 24, 779.
- Gao, H. X.; Jiang, T.; Han, B. X.; Wang, Y.; Du, J. M.; Liu, Z. M.; Zhang, J. L. *Polymer* 2004, 45, 3017.
- Campos, T. L. A.; Kersting, D. F.; Ferreira, C. A. *Surf Coat Technol* 1999, 122, 3.
- Chan, H. S. O.; Teo, M. T. B.; Khor, E.; Lim, C. N. *J Thermal Anal* 1989, 35, 765.
- Neoh, K. G.; Kang, E. T.; Tan, K. L. *Thermochim Acta* 1990, 171, 279.
- Oh, S. Y.; Kop, H. C.; Choi, J. W.; Rhee, H. W.; Kim, H. S. *Polym J* 1997, 29, 404.
- Wei, Y.; Hsueh, K. F. *J Polym Sci Part A: Polym Chem* 1989, 27, 4351.